Glycobiology vol. 18 no. 6 pp. 483–491, 2008
doi:10.1093/glycob/cwn028
Advance Access publication on March 31, 2008

A simplified and sensitive fluorescent method for disaccharide analysis of both heparan sulfate and chondroitin/dermatan sulfates from biological samples

Jon A Deakin and Malcolm Lyon[1]

Cancer Research UK Glyco-Oncology Group, School of Cancer and Imaging Sciences, University of Manchester, Paterson Institute for Cancer Research, Manchester M20 4BX, UK

Received on February 7, 2008; revised on March 13, 2008; accepted on March 26, 2008

Sulfated glycosaminoglycans regulate the biological functions of a wide variety of proteins, primarily through high affinity interactions mediated by specific sugar sequences or patterns/densities of sulfation. Disaccharide analysis of such glycosaminoglycans yields important diagnostic and comparative structural information on sulfate patterning. When applied to specific oligosaccharides it can also make a vital contribution to sequence elucidation. Standard UV detection of lyase-generated disaccharides resolved by HPLC can lack sufficient sensitivity and be compromised by contaminating UV signals, when dealing with scarce tissue- or cell culture-derived material. Various methods exist for improved detection, but usually involve additional HPLC hardware and often necessitate different procedures for analyzing different glycosaminoglycans. We describe a simple procedure, requiring only standard HPLC instrumentation, involving prederivatization of disaccharides with 2-aminoacridone with no cleanup of samples, followed by a separation by reverse-phase HPLC that is sensitive to as little as ∼100 pg (∼10^{-13} mol) of an individual disaccharide, thereby allowing analyses of >10 ng of total glycosaminoglycan. Importantly, separate analysis of both HS/heparin and CS/DS species within a mixed glycosaminoglycan pool can be performed using the same procedure on a single column. We demonstrate its applicability in dealing with small quantities of material derived from rat liver (where we demonstrate a high abundance of the unusual CS-E species within the CS/DS pool) and MDCK cells (which revealed a HS species of relatively low *N*-sulfation, but high *O*-sulfation). This simplified method should find a widespread utility for analyzing glycosaminoglycans from limited animal and cell culture samples.

Keywords: Chondroitin sulfate/dermatan sulfate/disaccharides/glycosaminoglycans/heparan sulfate

Introduction

The major sulfated glycosaminoglycan (GAG) components of proteoglycans (PGs), namely heparan sulfate (HS)/heparin and chondroitin sulfate (CS)/dermatan sulfate (DS), are complex linear polysaccharides. They are constructed initially of repeating disaccharide units of β-D-glucuronate (GlcA) linked to either α-D-*N*-acetylglucosamine (GlcNAc), in HS/heparin, or β-D-*N*-acetylgalactosamine (GalNAc), in CS/DS. These repeating units can then be subjected to considerable postpolymeric modification, i.e. epimerization of some GlcA to α-L-iduronate (IdoA), and sulfation to varying degrees at a number of potential monosaccharide and ring positions, to yield a variety of potential disaccharide structures. In HS/heparin, sulfation predominantly occurs at C2 of IdoA and the N- and C6-positions of hexosamine (and rarely at C3); in CS/DS it can occur at C4 or C6 of GalNAc as well as C2 of IdoA. Such qualitative and quantitative variations give rise to complex GAGs that can differ in composition and sequence, in a regulated manner, between cell types, tissues, and animal species (for a recent review see Bulow and Hobert 2006).

The biological activities of complex GAGs are intimately related to their structural diversity and ability to interact with many cell surface and extracellular proteins, thereby modifying their behavior. Such interactions are mostly driven by the recognition of patterns of modification, which can vary in degree of specificity from highly specific sequences present in a single GAG subfamily (e.g., antithrombin-III binding to heparin/HS (Thunberg et al. 1982)) through to less specific levels or disposition of sulfation that can be satisfied by more than one GAG type (e.g., hepatocyte growth factor/scatter factor binding to both heparin/HS and DS (Catlow et al. 2008)). Appreciation of GAG composition and sequence is thus fundamental to understanding its protein recognition properties and biological function.

Although various sophisticated techniques have now been developed to enable sequence analysis of GAG oligosaccharides (reviewed by Merry et al. 2002), there continues to be a widespread need for simple disaccharide compositional analysis of GAGs and oligosaccharides. Such analysis has application in (i) characterizing GAGs from novel animal species, (ii) comparing GAGs from different tissues or cell cultures, (iii) analyzing the effects of experimentally induced changes in expression levels of biosynthetic enzymes or specific enzyme knock-outs, (iv) analyzing subpopulations of GAGs (or fragments) with differing protein affinities or biological properties in vitro, (v) evaluating the extent and specificity of specific chemical desulfations of GAGs used in determining protein-binding specificities, and (vi) aiding the sequencing of small oligosaccharides.

Quantitative fragmentation of GAGs to disaccharides is readily achieved using widely available bacterial lyases that conveniently introduce a C4–C5 double bond, with its attendant characteristic UV absorption, into the nonreducing terminal

[1]To whom correspondence should be addressed: Tel: +44-0161-446-3202; Fax: +44-0161-446-3269; e-mail: mlyon@picr.man.ac.uk

hexuronate residue of a released disaccharide. After separation on strong anion-exchange (SAX)-HPLC columns, such disaccharides can be readily detected by their absorption at 232 nm. This is convenient for submilligram quantities of samples that are relatively free of other significant, UV-absorbing components. However, many biological GAG samples are both much less abundant and much less UV clean, making such detection more problematic.

One alternative is to use more sensitive sugar detection systems such as pulsed amperometric detection (Midura et al. 1994), but at the cost of requiring additional specialist hardware. In some cases, especially for cell/tissue culture (Merry et al. 2001) and also occasionally in in vivo animal studies (Lyon et al. 1994), it is possible to resort instead to specific metabolic radiolabeling of GAGs. This gives a much increased level of detection sensitivity coupled with the invisibility of unlabeled contaminants. Though undoubtedly effective, this is both expensive, in terms of radioisotopes, and requires either in-line radioactivity detection (i.e., additional, expensive equipment) or manual fraction collection and liquid scintillation counting (the latter is time-consuming and thus often rate-limiting in terms of analytical through-put). Radioisotope usage is also not always practicable and frequently undesirable, in some laboratory environments.

A further alternative is to utilize the increased sensitivity that specific fluorescent labeling of disaccharides (either pre- or post-chromatography) can provide. A number of effective methods have been previously described, varying widely in ease of use, sensitivity and general applicability to different GAGs, samples, etc. Precolumn fluorescent tagging of disaccharides can be effective and, in some cases, can allow the continued use of anion exchange to effect separation (Plaas et al. 1996; Kinoshita and Sugahara 1999; Yamada et al. 2007), though, in other cases, the nature of the fluorescent tag may adversely affect their behavior on such columns. An alternative chromatographic separation that can sometimes provide better resolution is reverse-phase (RP)-HPLC, though this may also require strict temperature control of the column (Skidmore et al. 2006). As an alternative, postcolumn derivatization of already separated disaccharides allows retention of an existing successful chromatographic system; the disadvantage being that it requires integration into the HPLC setup of hardware for effecting the in-line postderivatization chemistry (Huang et al. 1996; Toyoda et al. 1999).

For utility, an ideal fluorescence methodology would thus be one based upon precolumn labeling (i.e., no additional hardware). Preferably it should not require pre- or postlabeling cleanup of the sample that could introduce losses of disaccharides and thus potentially distort the composition. For some labeling chemistries, the disaccharides must be purified before fluorescent tagging can be undertaken (Du and Eddington 2002), and for others the excess labeling reagents preferably need to be removed from the disaccharides before chromatographic analysis, as their elution can mask disaccharide peaks (Kinoshita and Sugahara 1999; Yamada et al. 2007). Finally, it is often the case that prederivatization procedures have been developed and optimized for the analysis of a single GAG type, such that analysis of a different GAG may require switching of methodologies. An ideal methodology should be one that is equally applicable, with little or no modification, to the analysis of all major sulfated GAG types.

We demonstrate here that a combination of disaccharide derivatization with 2-aminoacridone (AMAC) without a need for a sample cleanup or removal of excess label, followed by a single-step C18 RP-HPLC chromatography running at room temperature, provides a high-resolution system that is effective in analyzing as little as 10 ng of either HS/heparin or CS/DS from animal tissues or cultured cells.

Results and discussion

Separation of fluorescent AMAC-labeled disaccharide standards by C18 RP-HPLC

GAG disaccharides can be readily derivatized at their reducing end by reductive amination with the AMAC fluorophore, as used for analysis of GAG–protein interactions by gel mobility shift assays (Lyon et al. 2004). The hydrophobic nature of fluorophores like AMAC can significantly alter the solution properties of the tagged disaccharides, leading to reduced chromatographic resolution on standard SAX-HPLC columns, compared to what can be achieved by, for example, capillary electrophoresis (Kitagawa et al 1995). However, AMAC disaccharides do chromatograph as sharp, symmetric peaks on a number of C18 RP-HPLC columns, when eluted with an increasing methanol gradient, with a better spread of peaks and less evidence of the clustering of disaccharide isomers that generally occurs with SAX-HPLC. By gradient optimization it was possible to fully resolve a mixture of eight HS/heparin disaccharides with baseline separation (Figure 1A). By contrast to SAX-HPLC (not shown), the disaccharides elute in a reverse order, i.e., trisulfated species first and nonsulfated species last. An identical gradient also resolves eight CS/DS disaccharides on the same column, though individually they elute noticeably later than similarly charged HS/heparin disaccharides (Figure 1B). Interestingly, this method gives baseline separation of the major isomeric ΔHexA-GalNAc(4S) and ΔHexA-GalNAc(6S) disaccharides, which is not always achieved by SAX-HPLC. Also, it fully resolves the minor ΔHexA(2S)-GalNAc disaccharide, whose presence cannot always be ascertained by SAX-HPLC, whether underivatized (data not shown) or fluorescently tagged (Kinoshita and Sugahara, 1999), as it tends to coelute underneath the major doublet of monosulfated disaccharides.

A major advantage of this protocol is that excess free AMAC is strongly retained by the RP column (elution time of >42 min; not shown), and thus does not have to be removed from samples prior to HPLC. However, a minor AMAC-related peak does elute earlier and distinctively (~24.5–25 min), within the disaccharide elution spectrum. Though much less abundant than free AMAC, this component can still be substantial when analyzing disaccharide levels within scarce biological samples. However, commercial AMAC can be effectively batch prepurified, if necessary, to remove the vast majority (>98%) of this component by a simple hydrophobic interaction chromatography step (as described in *Materials and Methods*; data not shown). When repurified AMAC is used for disaccharide labeling, the contaminant is then very substantially reduced giving a discrete peak that, when noticeable, is fully resolved from surrounding disaccharides (see Sensitivity of analysis compared with standard UV detection).

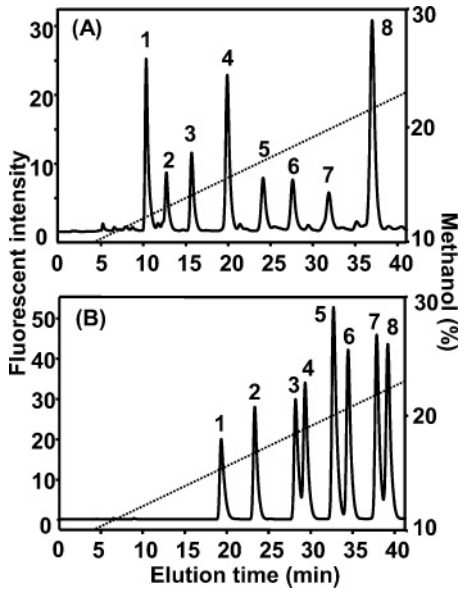

Fig. 1. Separation of AMAC-labeled disaccharide standards by RP-HPLC. Separate mixtures of eight HS/heparin disaccharides (**A**) or eight CS/DS disaccharides (**B**) were labeled with AMAC, resolved by C18 RP-HPLC, and detected by in-line fluorescence as described in *Materials and Methods*. In (**A**) the numbered disaccharide peaks correspond to 1, ΔHexA(2S)-GlcNS(6S); 2, ΔHexA-GlcNS(6S); 3, ΔHexA(2S)-GlcNS; 4, ΔHexA-GlcNS; 5, ΔHexA(2S)-GlcNAc(6S); 6, ΔHexA-GlcNAc(6S); 7, ΔHexA(2S)-GlcNAc; and 8, ΔHexA-GlcNAc. In (**B**) the numbered disaccharide peaks correspond to 1, ΔHexA(2S)-GalNAc(4S, 6S); 2, ΔHexA(2S)-GalNAc(4S); 3, ΔHexA(2S)-GalNAc(6S); 4, ΔHexA-GalNAc(4S, 6S); 5, ΔHexA(2S)-GalNAc; 6, ΔHexA-GalNAc(4S); 7, ΔHexA-GalNAc(6S); and 8, ΔHexA-GalNAc.

As with many chemical tagging procedures that target the reducing end of GAG oligosaccharides, the efficiency of labeling/detection is influenced by structural features adjacent to the reducing end. Thus, fluorescent peak areas do not directly correspond to the actual proportions of each disaccharide within a mixture, unlike with UV detection. In order to calculate appropriate correction factors for the specific fluorescent yields of different disaccharides, both HS/heparin and CS/DS disaccharides were analyzed by SAX-HPLC or RP-HPLC (4–6 replicates of each), as unlabeled or AMAC-labeled species, respectively, and the corresponding UV absorbance and fluorescent peak areas were compared. The most efficiently labeled HS/heparin and CS/DS disaccharides were ΔHexA(2S)-GlcNS(6S) and ΔHexA-GalNAc(4S, 6S), respectively, and these were assigned correction factors of 1.00. By comparison, all other fluorescent disaccharides required the application of correction factors (within the range of 1.05–2.28; Tables I and II), by which their respective peak areas should be multiplied to give their true relative abundance.

Sensitivity of analysis compared with standard UV detection

The effective sensitivity of disaccharide detection by UV is of the order of 100 ng ($\sim 10^{-10}$ mol), which means that disaccharide compositional analysis of GAGs (either HS/heparin or CS/DS) requires a minimum of 10 μg GAG, if minor disaccharides existing at frequencies of ∼1% are to be effectively quantified. Figure 2 illustrates the corresponding sensitivity of disaccharide analysis of porcine mucosal HS using AMAC

Table I. Correction factors for HS disaccharides

Peak number	Disaccharide structure	Correction factor[a]
1	ΔHexA(2S)-GlcNS(6S)	1.00
2	ΔHexA-GlcNS(6S)	1.07
3	ΔHexA(2S)-GlcNS	1.24
4	ΔHexA-GlcNS	1.37
5	ΔHexA(2S)-GlcNAc(6S)	1.47
6	ΔHexA-GlcNAc(6S)	1.51
7	ΔHexA(2S)-GlcNAc	2.09
8	ΔHexA-GlcNAc	2.04

[a]Each value is the average of six determinations. All values are expressed relative to ΔHexA(2S)-GlcNS(6S) which, as the most efficiently labeled, is set as 1.00.

Table II. Correction factors for CS/DS disaccharides

Peak number	Disaccharide structure	Correction factor[a]
1	ΔHexA(2S)-GalNAc(4S, 6S)	1.91
2	ΔHexA(2S)-GalNAc(4S)	2.28
3	ΔHexA(2S)-GalNAc(6S)	1.00
4	ΔHexA-GalNAc(4S, 6S)	1.37
5	ΔHexA(2S)-GalNAc	1.05
6	ΔHexA-GalNAc(4S)	1.47
7	ΔHexA-GalNAc(6S)	1.26
8	ΔHexA-GalNAc	1.52

[a]Each value is the average of four determinations. All values are expressed relative to ΔHexA(2S)-GalNAc(6S) which, as the most efficiently labeled, is set as 1.00.

labeling. With 10 μg of HS (i.e., the minimum for reasonable UV analysis) a very clean profile results that allows easy quantitation of the six disaccharides commonly encountered (Figure 2A; Table III). Fluorescence response is linear with the concentration up to at least 10 μg of an individual disaccharide (data not shown), and corresponding analyses of digests of as little as 10 ng of HS still yield an interpretable profile (Figure 2B). At the latter level of sensitivity the minor AMAC contaminant (peak X) becomes prominent, though it remains adequately resolved from surrounding disaccharides (Figure 2B). A very close correspondence of composition is observed for digests of 100 ng–10 μg of HS, and even the lower 10 ng still gives a broadly similar disaccharide composition, though the errors become noticeably larger at HS levels of ≤100 ng (Table III). Analyses of total integrated disaccharide peak areas (not shown) indicate that disaccharide yields across this wide range of HS substrate quantities remain quantitative, signifying a linearity of lyase digestion.

In the analysis of 10 ng of HS the content of a trisulfated disaccharide (peak 1) is approximately 200 pg ($\sim 2.5 \times 10^{-13}$ mol), and in reality ∼100 pg (10^{-13} mol) of an individual disaccharide is probably the workable limit of detection/quantitation. On this basis, the minimum quantity of GAG for analysis by this procedure (giving quantitation over a wide range of constituent disaccharide frequencies, down to ∼1% minimum abundance) would indeed be ∼10 ng. However, ∼50–100 ng of total HS may be preferable for improved signal-to-noise resolution and accuracy. Conversely, if the method is to be used for compositional analysis of a highly purified, small oligosaccharide species (maybe as an aid to sequencing), in which fewer disaccharide species are represented, and at more balanced frequencies, then the usable sensitivity could be reduced to a few ng of sample.

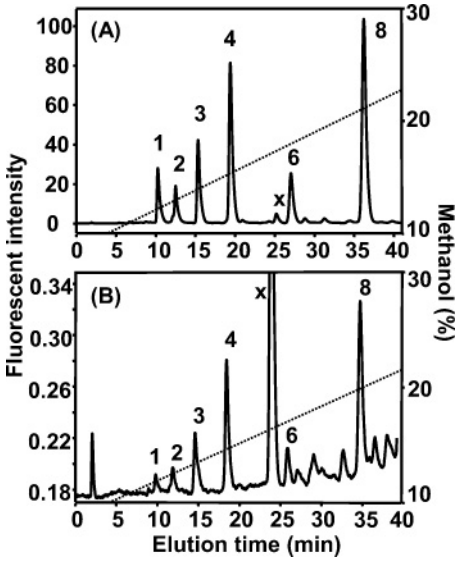

Fig. 2. Sensitivity of a disaccharide compositional analysis of HS. Porcine mucosal HS, either 10 μg (**A**) or 10 ng (**B**), was digested to disaccharides using a combination of heparinases. The disaccharides were then AMAC labeled, resolved by C18 RP-HPLC, and detected by fluorescence. Disaccharide peaks are numbered as described in the legend to Figure 1. Peak X corresponds to an AMAC-derived contaminant (*N.B.* this is dramatically enhanced in (**B**) compared to (**A**), as the same amount of AMAC was used for labeling, even though the quantity of HS was reduced 1000-fold).

Disaccharide analysis of rat liver PGs

Rat liver PGs, containing both HSPGs and CS/DS-PGs, were purified by the method of Lyon and Gallagher (1991) and digested with either chondroitinase ABC or a mix of heparinases I, II, and III. The resulting disaccharides were then either AMAC labeled and analyzed by RP-HPLC with fluorescent detection (Figure 3A and C) or analyzed in an underivatized form on SAX-HPLC with UV detection (Figure 3B and D).

In the HS disaccharide analysis the UV profile (50 μg HS) contained identifiable disaccharide peaks, but some peaks were clearly asymmetric and the baseline was poor, especially early in the profile (Figure 3B). UV analyses of impure samples, even when material is relatively abundant, are often limited by various factors. These include (i) baseline quality due to UV contaminants originating from both the enzymes as well as the sample, leading to the occurrence, and sometimes superimposition, of extraneous peaks in the early part of the gradient, principally around the elution position of the nonsulfated ΔHexA-GlcNAc, but sometimes extending as far as the ΔHexA-GlcNS disaccharide and (ii) the acute salt sensitivity of the nonsulfated disaccharide sometimes leading to splitting of this peak between nonretarded and weakly bound fractions. By contrast, the fluorescence profile (obtained from ∼0.7 μg of HS; Figure 3A) identified the same components on a much cleaner baseline, giving better quantitation (Table IV). The resulting highly sulfated composition was similar to that previously reported from analysis of rat liver HS that had been metabolically radiolabeled in vivo (Lyon et al. 1994) (Table IV). Indeed the results are surprisingly similar considering that the earlier analysis might have been expected to bias the analysis toward more recently synthesised HS, possibly produced by the most metabolically active cell population within the liver. However, it would now seem from the present results that the analysis obtained from metabolic radiolabeling was indeed a representative of the whole HS population.

Analysis of the CS/DS component from an equivalent aliquot of the rat liver PG pool indicated the presence of about three times more CS/DS (∼2 μg) than HS. The fluorescence profile (Figure 3C) indicated a composition dominated by the monosulfated ΔHexA-GalNAc(4S) disaccharide (71.3%), with relatively little monosulfated ΔHexA-GalNAc(6S) disaccharide (6.2%), but with an unusually high occurrence of the disulfated ΔHexA-GalNAc(4S, 6S) disaccharide (17%) (Table V). The latter structure, often referred to as the CS-E disaccharide, is the dominant component in squid cartilage CS. Such CS-E structures are also known to occur in the mammalian brain (Deepa et al. 2002; Purushothaman et al. 2007), but their presence in liver expands the known mammalian tissue distribution. Their surprising abundance, especially when compared to the relatively low occurrence of disulfated disaccharides containing

Table III. Disaccharide composition of porcine mucosal HS: comparison of analyses by UV and fluorescence detection over a range of HS digestion sizes

		Frequency (%)				
Peak number	HS disaccharide structure	UV[a] 10 μg HS	Fluorescence[b] 10 μg HS	1 μg HS	100 ng HS	10 ng HS
1	ΔHexA(2S)-GlcNS(6S)	5.4 (0.23)	4.1 (0.07)	3.7 (0.07)	3.3 (0.16)	2.5 (0.76)
2	ΔHexA-GlcNS(6S)	3.9 (0.35)	3.3 (0.03)	3.0 (0.14)	3.3 (0.24)	2.1 (0.10)
3	ΔHexA(2S)-GlcNS	10.4 (0.12)	8.6 (0.07)	8.4 (0.07)	9.4 (0.52)	8.3 (0.87)
4	ΔHexA-GlcNS	22.6 (0.78)	21.2 (0.36)	22.4 (0.14)	22.5 (0.67)	26.5 (0.17)
5	ΔHexA(2S)-GlcNAc(6S)	n.d.	n.d.	n.d.	n.d.	n.d.
6	ΔHexA-GlcNAc(6S)	8.6 (0.56)	9.0 (0.13)	9.2 (0.26)	8.5 (0.19)	6.4 (0.13)
7	ΔHexA(2S)-GlcNAc	n.d.	n.d.	n.d.	n.d.	n.d.
8	ΔHexA-GlcNAc	48.4 (0.40)	53.8 (0.39)	53.2 (0.14)	52.9 (1.18)	54.2 (1.5)
	Sulfation position					
	NS	42.3	37.2	37.6	38.5	39.4
	2S	15.8	16.4	15.9	15.1	11.0
	6S	17.9	12.7	12.2	12.7	10.8
	Total S	76.0	66.2	65.7	66.3	61.1

n.d.: not determined.
[a]Average of two determinations with standard error in parentheses.
[b]Average of three determinations with standard error in parentheses.

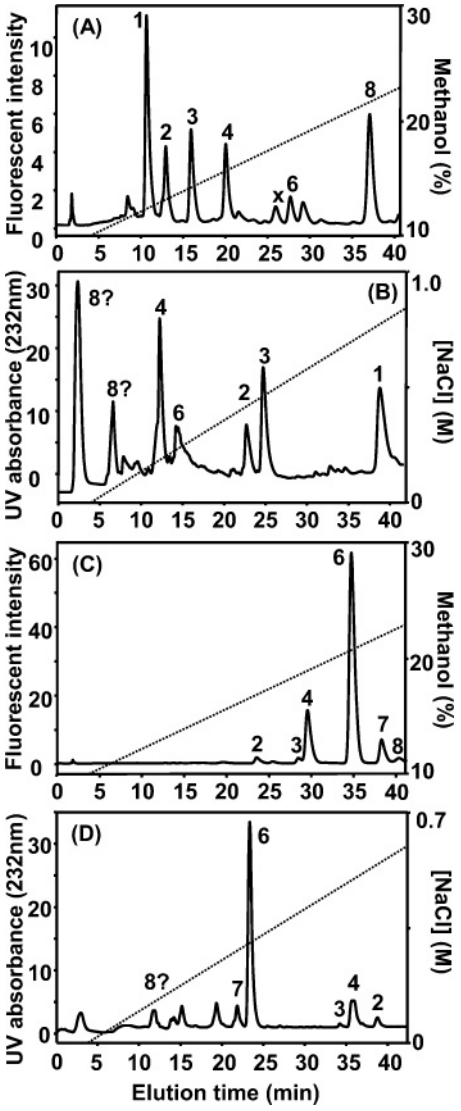

Fig. 3. Disaccharide analyses of GAGs from purified rat liver PGs. Component HSPGs or CS/DS-PGs were digested to disaccharides using a combination of heparinases (**A**, **B**) or chondroitinase ABC (**C**, **D**), respectively. Samples were either AMAC labeled, resolved by C18 RP-HPLC, and detected by fluorescence (**A**, **C**) or run underivatized on SAX-HPLC with UV detection (**B**, **D**). Disaccharide peaks are numbered as described in the legend to Figure 1.

2-*O*-sulfates, suggests a potentially interesting, though presently unknown, biological function in this organ.

In comparison with the fluorescence profile, the corresponding UV profile (Figure 3D) contained a number of peaks eluting in the early half of the profile that are unlikely to correspond to disaccharides. One of these, eluting at ~12 min, could easily be ascribed, though mistakenly, as corresponding to ΔHexA-GalNAc, a disaccharide that was shown by AMAC labeling to be very low (1.1%) in abundance (Figure 3D). This demonstrates the utility of the AMAC procedure in removing the uncertainties inherent in quantitation by UV analysis of nonsulfated disaccharides, in particular.

Disaccharide analysis of rat liver plasma membrane PGs

In order to test the ability of the method to deal with similar but less pure materials, plasma membranes prepared from rat liver were digested with Pronase, and the GAGs recovered by single-step elution from an anion-exchange column, and then enzyme digested for disaccharide analysis. Perfectly interpretable fluorescent profiles were again obtained (data not shown), though compositional differences were seen in both HS and CS/DS when compared with analyses of the corresponding GAGs from the purified liver PGs (Tables IV and V).

The membrane-associated CS/DS possessed an even higher sulfation level than that derived from the whole liver (138 versus 120 sulfates per 100 disaccharides), but still retained the diagnostic abundance of the disulfated CS-E-type disaccharide (Table V). However, it did contain a greater abundance of both the disulfated CS-B (ΔHexA(2S)-GalNAc(4S)) and trisulfated (ΔHexA(2S)-GalNAc(4S, 6S)) disaccharides (the overall abundance of 2-*O*-sulfated disaccharides being similar to that of CS-E disaccharides). These differences between total liver and plasma membrane pools may suggest that a specific subpopulation of the total liver CS/DS is extrinsically associated with the plasma membrane and that this association may be enhanced specifically by enrichment with 2-*O*-sulfation (i.e., a more DS-like species).

In contrast, the plasma membrane-derived HS had a substantially lower overall sulfation level than the total liver PG-derived HS, with a particular enhancement of the nonsulfated (ΔHexA-GlcNAc) disaccharide component (Table IV). These differences could reflect the presence of a heterogeneous HS population in the liver, maybe contributed by different cell types with different cell surface and extracellular distributions. The radically different purification protocols may differentially select HS subsets of this population with different average compositions. However, there may be an alternative explanation. It is documented that there is a potent heparanase-like activity associated with purified liver plasma membranes (Gallagher et al. 1988) that rapidly liberates fragments of HS from plasma membranes upon their transfer from a high concentration of sucrose (inhibitory to the enzyme) to PBS. The rat liver HS chain has a highly asymmetric structure in which an extended nonsulfated region is proximal to the protein core, whereas its extensive sulfation is concentrated toward its distal, nonreducing end (Lyon et al. 1994). Any heparanase-mediated chain cleavage that occurred prior to Pronase extraction would thus enrich the membrane-bound fraction with shorter, less-sulfated chains, thereby elevating, principally, the level of ΔHexA-GlcNAc disaccharides and reciprocally reducing overall sulfation, as is indeed the case (Table IV).

Disaccharide analyses of MDCK cell culture GAGs

A particular challenge is to readily analyze GAGs isolated from cell cultures, where metabolic radiolabeling has frequently been the method of choice to provide the requisite sensitivity. Here we have separately analyzed HS and CS/DS in a mixed GAG pool partially purified from a total MDCK cell culture. GAGs equivalent to that produced by approximately one 10-cm dish of ~50% confluent cells were analyzed and gave clean and interpretable compositions (Figure 4 and Table VI). This indicates the further scope for significant reduction in the number of cells that could be analyzed. By contrast, equivalent analyses attempted using direct UV detection were lacking in sensitivity and of very poor quality (date not shown). It is important to note, in this context, that in order to analyze CS/DS

Table IV. HS disaccharide compositions of PGs purified from whole rat liver versus a partially purified GAG pool from rat liver plasma membranes

Peak number	HS disaccharide structure	Frequency (%)			
		PG (radiolabel)[a]	PG (UV)	PG (fluor.)	Plasma membranes (fluor.)[b]
1	ΔHexA(2S)-GlcNS(6S)	19.8	18.6	22.0	9.7 (0.4)
2	ΔHexA-GlcNS(6S)	5.2	6.2	9.4	5.3 (0.4)
3	ΔHexA(2S)-GlcNS	15.1	14.5	14.3	11.6 (1.2)
4	ΔHexA-GlcNS	18.8	16.4	12.6	18.9 (1.0)
5	ΔHexA(2S)-GlcNAc(6S)	0.5	n.d.	n.d.	n.d.
6	ΔHexA-GlcNAc(6S)	6.5	4.6	5.2	6.3 (0.6)
7	ΔHexA(2S)-GlcNAc	1.3	n.d.	n.d.	n.d.
8	ΔHexA-GlcNAc	32.8	39.7	36.7	48.2 (3.7)
	Sulfation position				
	NS	58.9	55.7	58.3	45.5
	2S	36.7	33.1	36.3	21.3
	6S	32.0	29.4	36.6	21.3
	Total S	127.6	118.2	131.2	88.1

n.d.: not determined.
[a]Determined by radiochemical detection of disaccharides from [^{3}H]HSPG obtained from rat liver after metabolic radiolabeling with D-[6-^{3}H] glucosamine hydrochloride, as previously published by Lyon et al. (1994).
[b]Average of two determinations with standard error in parentheses.

composition, any hyaluronan within a tissue or cell extract must be rigorously removed, as accomplished here using a 0.25 M NaCl wash of the DEAE-Sephacel column prior to the recovery of the sulfated GAGs. Any contaminating hyaluronan present will also be degraded by chondroitinase ABC, yielding an abundance of the nonsulfated ΔHexA-GlcNAc disaccharide. The latter will be indistinguishable chromatographically from ΔHexA-GalNAc derived genuinely from CS/DS, which is usually a relatively minor component and could thus be easily overwhelmed inadvertently. Using the above hyaluronan removal procedure only 1.1% and 0.7% of ΔHexA-GalNAc were detected in rat liver and MDCK CS/DS, respectively.

This novel analysis of MDCK HS revealed it to possess a typical overall sulfation level (84.9 sulfates/100 disaccharides), when compared to a range of HS species (Gallagher and Walker 1985) (Figure 4A and Table VI). However, this sulfate density comprises an unusually low level of *N*-sulfation (38.1/100 disaccharides) coupled to a relatively high level of *O*-sulfation (46.8/100 disaccharides), i.e. an *O*-sulfate/*N*-sulfate ratio of 1.23 (for most HS species this ratio is usually <1; Gallagher and Walker 1985). Ignoring the proportion of 6-*O*-sulfation which is present on GlcNAc residues, the relatively sparse S-domains in MDCK HS will thus be highly sulfated overall (∼2 sulfates/disaccharide on average) and indeed 36% of its *N*-sulfated disaccharides are seen to be trisulfated (Table VI).

Analysis of the CS/DS component of MDCK cells revealed almost twice as much 6-*O*-sulfation as 4-*O*-sulfation (Figure 4B and Table VI). A significant minority (∼12%) of disaccharides are 2-*O*-sulfated, present as both 2-*O*/4-*O* and 2-*O*/6-*O*- disulfated disaccharides but, in contrast to the rat liver CS/DS, there are very few (∼1%) CS-E disaccharides. Clearly a significant DS component may be present, though such a compositional analysis alone is insufficient for estimating the actual proportions of CS versus DS chains in the total CS/DS pool.

In summary, we have demonstrated the utility of a single, simple, and sensitive fluorescence-based analysis, requiring only standard HPLC technology, which is equally applicable, without modification, for both HS and CS/DS. The method copes

Table V. CS/DS disaccharide compositions of PGs purified from whole rat liver versus a partially purified GAG pool from rat liver plasma membranes

Peak number	CS/DS disaccharide structure	Frequency (%)		
		PG (UV)	PG (fluor.)	Plasma membranes (fluor.)[a]
1	ΔHexA(2S)-GalNAc(4S, 6S)	n.d	0.6	5.4 (2.4)
2	ΔHexA(2S)-GalNAc(4S)	3.6	2.8	8.7 (2.3)
3	ΔHexA(2S)-GalNAc(6S)	0.9	1.0	3.0 (1.2)
4	ΔHexA-GalNAc(4S, 6S)	15.5	17.0	15.4 (0.4)
5	ΔHexA(2S)-GalNAc	n.d.	n.d.	n.d.
6	ΔHexA-GalNAc(4S)	72.4	71.3	62.4 (3.7)
7	ΔHexA-GalNAc(6S)	7.5	6.2	5.0 (1.2)
8	ΔHexA-GalNAc	n.d.	1.1	n.d.
	Sulfation position			
	4S	91.5	91.7	91.9
	6S	23.9	24.8	28.8
	2S	4.5	4.4	17.1
	Total S	119.9	120.9	137.8

n.d.: not determined.
[a]Average of two determinations with standard error in parenthesis.

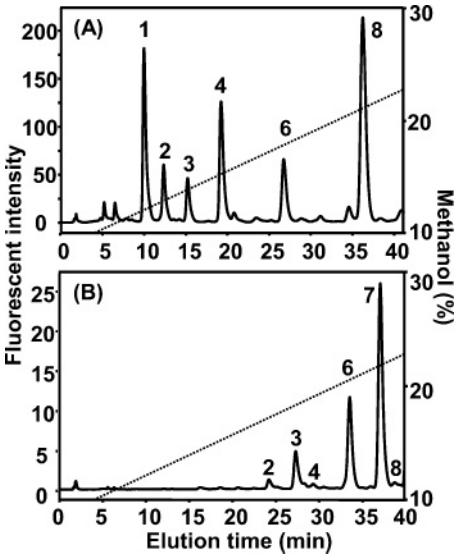

Fig. 4. Disaccharide analyses of GAGs from MDCK cell cultures. The HS and CS/DS components of the GAG pool, released from MDCK cell culture PGs by proteolysis, were digested to disaccharides using (**A**) a combination of heparinases or (**B**) chondroitinase ABC, respectively. Samples were AMAC–labeled, resolved by C18 RP-HPLC, and detected by fluorescence. Disaccharide peaks are numbered as described in the legend to Figure 1.

well with biological samples of both tissue- and cell-culture origins. Presently, this methodology is finding considerable application in our own laboratory for analyzing GAGs that are in limited supply, from either human tissues or stem cell cultures, and should find a wide application in a variety of laboratories equipped with basic HPLC facilities.

Materials and methods

Materials

AMAC and DEAE-Sephacel were supplied by Sigma (Poole, UK). Porcine intestinal mucosal HS was from NV Organon (Oss, The Netherlands). Chondroitinase ABC (*Proteus vulgaris*; EC 4.2.2.4) was purchased from AMS Biotechnology (Abingdon, UK). Heparinases I (*Pedobacter heparinus*; EC 4.2.2.7), II (P. *heparinus*; no EC number assigned), and III (P. *heparinus*; EC 4.2.2.8) were from Grampian Enzymes (Harray, Orkney, UK). The six major HS/heparin disaccharides were produced in-house. A complete range of eight CS/DS disaccharide standards and two less-common HS disaccharide standards (ΔHexA(2S)-GlcNAc and ΔHexA(2S)-GlcNAc(6S)) were obtained from Iduron (Manchester, UK). Prepacked PD-10 desalting columns were purchased from Amersham Biosciences (Chalfont St. Giles, UK). Cell culture media and sera were from Invitrogen (Paisley, UK).

Repurification of AMAC

AMAC (10 mg) dissolved in 1 mL of 85% DMSO/15% acetic acid was diluted to 5 mL with distilled water and loaded onto an Econo-Pac Macro-Prep *t*-butyl hydrophobic interaction chromatography column (2 mL bed volume; Bio-Rad Laboratories, Hemel Hempstead, UK) equilibrated in water. After a wash with 20 mL of 20% methanol to elute contaminants, the bound AMAC was step-eluted with 100% methanol. The methanol was then removed by evaporation and the pure AMAC was redissolved in 85% DMSO/15% acetic acid and stored at −20°C in the dark until use.

Enzymatic digestion of HS and CS/DS species to disaccharides

HS species were completely digested to disaccharides using 5 mIU each of a mix of heparinases I, II, and III in 50 μL of 0.1 M sodium acetate and 0.1 mM calcium acetate, pH 7.0, at 37°C overnight. CS/DS species were digested with 5 mIU of chondroitinase ABC in 50 μL of 50 mM Tris–acetate, pH 7.5. All digests were then dried down by centrifugal evaporation/freeze-drying.

AMAC labeling of disaccharides

Dried disaccharide standards or enzyme digests of GAGs (as above) were redissolved in 10 μL of 0.1 M AMAC in 85% DMSO/15% acetic acid and incubated at room temperature for 20 min. At this point, 10 μL of 1 M sodium cyanoborohydride was added and the mixture was left for 18 h at room temperature (∼20°C). Once labeled, samples do not need to be analyzed immediately as they are stable if stored in the dark, preferably frozen for a longer term storage.

Table VI. Disaccharide compositions of HS and CS/DS in a total GAG pool from MDCK cells

Peak number	HS disaccharide structure	Frequency (%)	Peak number	CS/DS disaccharide structure	Frequency (%)
1	ΔHexA(2S)-GlcNS(6S)	13.7	1	ΔHexA(2S)-GalNAc(4S, 6S)	0.8
2	ΔHexA-GlcNS(6S)	4.8	2	ΔHexA(2S)-GalNAc(4S)	3.5
3	ΔHexA(2S)-GlcNS	4.4	3	ΔHexA(2S)-GalNAc(6S)	8.0
4	ΔHexA-GlcNS	15.2	4	ΔHexA-GalNAc(4S, 6S)	1.2
5	ΔHexA(2S)-GlcNAc(6S)	n.d.	5	ΔHexA(2S)-GalNAc	n.d
6	ΔHexA-GlcNAc(6S)	10.2	6	ΔHexA-GalNAc(4S)	29.6
7	ΔHexA(2S)-GlcNAc	n.d.	7	ΔHexA-GalNAc(6S)	56.3
8	ΔHexA-GlcNAc	51.8	8	ΔHexA-GalNAc	0.7
	Sulfation position			Sulfation position	
	NS	38.1		4S	35.1
	2S	18.1		6S	66.3
	6S	28.7		2S	12.3
	Total S	84.9		Total S	113.7

n.d.: not determined.

SAX-HPLC separation of disaccharides

HS/heparin or CS/DS disaccharides were applied to Propac PA1 SAX-HPLC (4.6 mm × 250 mm; Dionex, Camberley, UK) or Sphereclone 5 μm SAX-HPLC (4.6 mm × 250 mm; Phenomenex, Macclesfield, UK) columns, respectively, running on an Agilent 1100 Series HPLC system. Both columns were pre-equilibrated in water acidified to pH 3.5 by titration with HCl, and after sample loading they were briefly washed again with pH 3.5 water. Disaccharide elution was effected using 45 mL linear gradients of 0–0.7 M NaCl, pH 3.5 (for CS/DS), or 0–1.0 M NaCl, pH 3.5 (for HS/heparin), at a flow rate of 1 mL/min. Disaccharides were detected by in-line UV absorption at 232 nm.

RP-HPLC separation of AMAC-labeled disaccharides

AMAC-labeled HS/heparin or CS/DS disaccharides (20 μL) were diluted with water to a final volume of 0.2 mL and applied to a Zorbax Eclipse XDB-C18 RP-HPLC column (4.6 mm × 150 mm; Agilent Technologies, Stockport, UK) equilibrated in 0.1 M ammonium acetate (solution A), running on an Agilent 1100 Series HPLC system. After a short and steep 2 mL gradient of 0–10% solution B (100% methanol), the disaccharides were then eluted over a shallow 50 mL linear gradient of 10–30% solution B at a flow rate of 1 mL/min. Disaccharides were detected by in-line fluorescence (excitation at 425 nm and emission at 520 nm). The column was finally regenerated by washing with 100% solution B before returning to solution A.

Partial purification of rat liver PGs and GAGs

Two different approaches were taken to provide alternative PG/GAG preparations of differing purity for disaccharide analysis. In one approach, total PGs were extracted under dissociative conditions (4 M guanidinium chloride, 2% Triton X-100) from a rat liver homogenate, and then purified, essentially as described by Lyon and Gallagher (1991). However, the PG preparation was not digested with chondroitinase ABC, as described therein, so as to retain the CS/DS-PG component. In the second approach, rat liver plasma membranes were prepared from rat liver homogenates by discontinuous sucrose centrifugation, as described in Gallagher et al. (1988). Membranes were pelleted out of sucrose by centrifugation at 12,000 rpm for 5 min, briefly washed with PBS, repelleted, and then suspended in 1 mL of PBS containing 1% Triton X-100 and digested with 1 mg/mL Pronase for 1 h at 37°C. The supernatant, recovered by centrifugation, was loaded onto a 1 mL DEAE-Sephacel column, which was then washed extensively with 0.25 M NaCl and 10 mM phosphate, pH 7.4, to remove hyaluronan and most non-GAG components. Bound sulfated GAGs were step-eluted with 1.5 M NaCl and 10 mM phosphate, pH 7.4, then desalted on a PD-10 column eluted with water, and finally freeze-dried.

The concentration of HS in the PG stock was analyzed by exhaustive digestion to disaccharides using a mixture of heparinases I, II, and III with monitoring of the consequent increase in absorbance at 232 nm. The concentration of disaccharide was calculated using a molar absorption coefficient of 5200 M^{-1} cm^{-1} (Linhardt et al. 1988) and an average disaccharide M_r calculated from its composition (Lyon et al. 1994).

Extraction and partial purification of GAGs from MDCK cell cultures

MDCK cells were grown in 10-cm-diameter plastic dishes in DMEM with 5% fetal calf serum at 37°C until approximately 50% confluent. The culture medium was then removed and the cell layers were solubilized in 5 mL per dish of PBS containing 1% Triton X-100 at room temperature for 1 h. The extracts were centrifuged at 2500 rpm for 10 min, the supernatants recovered and then combined with the reserved culture media. After digestion with 1 mg/mL Pronase at 37°C for 1 h, the sample was passed through a 5 mL DEAE-Sephacel column equilibrated with PBS. After an extensive wash with 0.25 M NaCl and 10 mM sodium phosphate, pH 7.0, to remove hyaluronan and most non-GAG components, the sulfated GAGs were recovered by step elution with 1.5 M NaCl and 10 mM sodium phosphate, pH 7.0. The eluant was desalted on a PD-10 column running in distilled water, and then freeze-dried.

Funding

This research was supported by Programme Grant funding from Cancer Research UK.

Acknowledgements

We would like to thank Dr Ermanno Gherardi (MRC Centre, Cambridge, UK) for kind provision of the MDCK cell line. We also thank Professor John Gallagher (University of Manchester, UK) for useful comments on the manuscript.

Conflict of interest statement

None declared.

Abbreviations

AMAC, 2-aminoacridone; CS, chondroitin sulfate; DMSO, dimethylsulfoxide; DS, dermatan sulfate; GAG, glycosaminoglycan; GalNAc, β-D-*N*-acetylgalactosamine; GlcA, β-D-glucuronic acid; GlcNAc, α-D-*N*-acetylglucosamine; GlcNS, α-D-*N*-sulfoglucosamine; HPLC, high performance liquid chromatography; HS, heparan sulfate; IdoA, α-L-iduronic acid; MDCK, Madin–Darby canine kidney; NS, *N*-sulfate; PG, proteoglycan; RP, reverse phase; SAX, strong anion exchange; ΔHexA, $\Delta^{4,5}$-unsaturated hexuronate residue generated by lyase cleavage of hexosaminidic linkage; 2S, 2-*O*-sulfate; 4S, 4-*O*-sulfate; 6S, 6-*O*-sulfate.

References

Bulow HE, Hobert O. 2006. The molecular diversity of glycosaminoglycans shapes animal development. *Annu Rev Cell Dev Biol*. 22:375–407.

Catlow KR, Deakin JA, Wei Z, Delehedde M, Fernig DG, Gherardi E, Gallagher JT, Pavão MSG, Lyon M. 2008. Interactions of hepatocyte growth factor/scatter factor with various glycosaminoglycans reveal an important interplay between the presence of iduronate and sulfate density. *J Biol Chem*. 283:5235–5248.

Deepa SS, Umehara Y, Higashiyama S, Itoh N, Sugahara K. 2002. Specific molecular interactions of oversulfated chondroitin sulfate E with various

heparin-binding growth factors: Implications as a physiological binding partner in the brain and other tissues. *J Biol Chem*. 277:43707–43716.

Du JP, Eddington N. 2002. Determination of the chondroitin sulfate disaccharides in dog and horse plasma by HPLC using chondroitinase digestion, precolumn derivatization, and fluorescence detection. *Anal Biochem*. 306:252–258.

Gallagher JT, Walker A. 1985. Molecular distinctions between heparan sulphate and heparin. Analysis of sulphation patterns indicates that heparan sulphate and heparin are separate families of *N*-sulphated polysaccharides. *Biochem J*. 230:665–674.

Gallagher JT, Walker A, Lyon M, Evans WH. 1988. Heparan sulphate – degrading endoglycosidase on liver plasma membranes. *Biochem J*. 250:719–726.

Huang Y, Washio Y, Hara M, Toyoda H, Koshiishi I, Toida T, Imanari T. 1996. Simultaneous determination of dermatan sulfate and oversulfated dermatan sulfate in plasma by high-performance liquid chromatography with post-column fluorescence derivatization. *Anal Biochem*. 240:227–234.

Kinoshita A, Sugahara K. 1999. Microanalysis of glycosaminoglycan-derived oligosaccharides labelled with a fluorophore 2-aminobenzamide by high-performance liquid chromatography: Application to disaccharide composition analysis and exosequencing of oligosaccharides. *Anal Biochem*. 269:367–378.

Kitagawa H, Kinoshita A, Sugahara K. 1995. Microanalysis of glycosaminoglycan-derived oligosaccharides labelled with the fluorophore 2-aminoacridone by capillary electrophoresis and high-performance liquid chromatography. *Anal Biochem*. 232:114–121.

Linhardt RJ, Rice KG, Kim YS, Lohse DL, Wang HM, Loganathan D. 1988. Mapping and quantification of the major oligosaccharide components of heparin. *Biochem J*. 254:781–787

Lyon M, Deakin JA, Gallagher JT. 1994. Liver heparan sulphate structure: A novel molecular design. *J Biol Chem*. 269:11208–11215.

Lyon M, Deakin JA, Lietha D, Gherardi E, Gallagher JT. 2004. The interactions of hepatocyte growth factor/scatter factor and its NK1 and NK2 variants with glycosaminoglycans using a modified gel mobility shift assay: Elucidation of the minimal size of binding and activatory oligosaccharides. *J Biol Chem*. 279:43560–43567.

Lyon M, Gallagher JT. 1991. The purification and partial characterisation of the major cell-associated heparan sulphate proteoglycans of rat liver. *Biochem J*. 273:415–422.

Merry CLR, Bullock SL, Swan DC, Lyon M, Beddington RSP, Wilson VA, Gallagher JT. 2001. The molecular phenotype of heparan sulphate in the HS2st$^{-/-}$ mutant mouse. *J Biol Chem*. 276:35429–35434.

Merry CLR, Lyon M, Gallagher JT. 2002. Sequencing of heparin and heparan sulfate oligosaccharides. In: Volpi N, editor. *Analytical Techniques to Evaluate the Structure and Function of Natural Polysaccharides, Glycosaminoglycans*. Trivandrum (India): Research Signpost. p. 129–142.

Midura RJ, Salustri A, Calabro A, Yanagishita M, Hascall VC. 1994. High-resolution separation of disaccharide and oligosaccharide alditols from chondroitin sulphate, dermatan sulphate and hyaluronan using CarboPac PA1 chromatography. *Glycobiology*. 4:333–342.

Plaas AHK, Hascall VC, Midura RJ. 1996. Ion-exchange HPLC microanalysis of chondroitin sulfate: Quantitative derivatization of chondroitin lyase digestion products with 2-aminopyridine. *Glycobiology*. 6:823–829.

Purushothaman A, Fukuda J, Mizumoto S, ten Dam GB, van Kuppevelt TH, Kitagawa H, Mikami T, Sugahara K. 2007. Functions of chondroitin sulfate/dermatan sulfate chains in brain development: Critical roles of E and iE disaccharide units recognised by a single chain antibody GD3G7. *J Biol Chem*. 282:19442–19452.

Skidmore MA, Guimond SE, Dumax-Vorzet AF, Atrih A, Yates EA, Turnbull JE. 2006. High sensitivity separation and detection of heparan sulfate disaccharides. *J Chromatogr A*. 1135:52–56.

Thunberg L, Bäckström G, Lindahl U. 1982. Further characterization of the antithrombin-binding sequence in heparin. *Carbohydr Res*. 100:393–410.

Toyoda H, Yamamoto H, Ogino N, Toida T, Imanari T. 1999. Rapid and sensitive analysis of disaccharide composition in heparin and heparan sulfate by reversed-phase ion-pair chromatography on a 2 μm porous silica gel column. *J Chromatogr A*. 830:197–201.

Yamada S, Morimoto H, Fujisawa T, Sugahara K. 2007. Glycosaminoglycans in *Hydra magnipapillata* (Hydrozoa, Cnidaria): Demonstration of chondroitin in the developing nematocyst, the sting organelle, and structural characterization of glycosaminoglycans. *Glycobiology*. 17:886–894.